Numerical Inversion of the Abel Integral Equation using Homotopy Perturbation Method

Sunil Kumar and Om P. Singh

Department of Applied Mathematics, Institute of Technology, Banaras Hindu University, Varanasi -221005, India

Reprint requests to O. P. S.; E-mail: singhom@gmail.com

Z. Naturforsch. **65a,** 677 – 682 (2010); received November 11, 2009 / revised December 10, 2009

Many problems in physics like reconstruction of the radially distributed emissivity from the line-of-sight projected intensity, the 3-D image reconstruction from cone-beam projections in computerized tomography, etc. lead naturally, in the case of radial symmetry, to the study of Abel's type integral equation. The aim of this communication is to propose a new algorithm for the Abel inversion by using the homotopy perturbation method.

Key words: Abel's Inversion; Homotopy Perturbation Method.

1. Introduction

Abel's integral equation [1] occurs in many branches of science. The earliest application, due to Mach [2], arose in the study of compressible flows around axially symmetric bodies. Usually, physical quantities accessible to measurement are quite often related to physically important but experimentally inaccessible ones by Abel's integral equation. In flame and plasma diagnostics the Abel integral equation

$$I(y) = 2\int_y^1 \frac{\varepsilon(r)r}{\sqrt{r^2-y^2}}\mathrm{d}r, \quad 0 \le y \le 1, \qquad (1)$$

relates the emission coefficient distribution function of optically thin cylindrically symmetric extended radiation source to the line-of-sight radiance measured in the laboratory. Obtaining the physically relevant quantity from the measured one requires, therefore, the inversion of the Abel integral, and in case the object does not have radial symmetry, it requires, in principal, the inversion of Radon transform.

Equation (1) is inverted analytically by [3]

$$\varepsilon(r) = -\frac{1}{\pi}\int_r^1 \frac{1}{\sqrt{y^2-r^2}}\frac{\mathrm{d}I(y)}{\mathrm{d}(y)}\mathrm{d}y, \quad 0 \le r \le 1. \qquad (2)$$

As the process of estimating the solution function (emissivity) $\varepsilon(r)$, if the data function (projected intensity) $I(y)$ is given approximately and only at a discrete set of data points, is ill-posed since even very small, high frequency errors in the measured $I(y)$, such as will arise from experimental errors, photon counting noise, and noise in the electronics, might cause large errors in the reconstructed solution $\varepsilon(r)$. This is due to the fact that the formula (2) requires differentiating the measured data. In fact, two explicit analytic inversion formulae were given by Abel [1], but their direct application amplifies the experimental noise inherent in the radiance data significantly [4]. In 1982, a third, analytic but derivative free, inversion formula was obtained by Deutsch and Beniaminy [5] to avoid this problem. In addition, many numerical inversion methods [5 – 14] have been developed with varying degree of success with the inherent limitations of all measured data. Consequently, the direct use of (2) is restricted and numerical methods become important.

The aim of the present paper is to present and analyse a new algorithm for the numerical solution of Abel's integral equation by using the homotopy perturbation method (HPM).

2. Basic Idea of Homotopy Perturbation Method

In this method, using the homotopy technique of topology, a homotopy is constructed with an embedding parameter $p \in [0,1]$ which is considered as a 'small parameter'. This method became very popular amongst the scientists and engineers, even though it involves continuous deformation of a simple problem into the more difficult problem under consideration. Most of the perturbation methods depend on the existence of a small perturbation parameter but many nonlinear problems have no small perturbation parameter at all. Many new methods have been proposed in the late nineties to solve such nonlinear equations devoid of such small parameters [15 – 18]. Late 1990s saw a surge in applications of homotopy theory in the scientific and engineering computations [19 – 22]. When the homotopy theory is coupled with the perturbation theory it provides a powerful mathematical tool [23 – 25]. A review of recently developed methods of nonlinear analysis can be found in [26]. To illustrate the basic concept of the homotopy perturbation method (HPM), consider the following nonlinear functional equation:

$$A(u) = f(r), \quad r \in \Omega \text{ with the boundary conditions } B\left(u, \frac{\partial u}{\partial n}\right) = 0, \quad r \in \partial\Omega, \tag{3}$$

where A is a general functional operator, B is a boundary operator, $f(r)$ is a known analytic function, and $\partial\Omega$ is the boundary of the domain Ω. The operator A is decomposed as $A = L + N$, where L is the linear and N is the nonlinear operator. Hence, (3) can be written as

$$L(u) + N(u) - f(r) = 0, \quad r \in \Omega.$$

We construct a homotopy $v(r, p) : \Omega \times [0,1] \to R$ satisfying

$$H(v, p) = (1-p)[L(v) - L(u_0)] + p[A(v) - f(r)] = 0, \quad p \in [0,1], \quad r \in \Omega. \tag{4}$$

Hence,

$$H(v, p) = L(v) - L(u_0) + pL(u_0) + p[N(v) - f(r)] = 0, \tag{5}$$

where u_0 is an initial approximation for the solution of (3). As

$$H(v, 0) = L(v) - L(u_0) \text{ and } H(v, 1) = A(v) - f(r), \tag{6}$$

it shows that $H(v, p)$ continuously traces an implicitly defined curve from a starting point $H(u_0, 0)$ to a solution $H(v, 1)$. The embedding parameter p increases monotonously from zero to one as the trivial linear part $L(u) = 0$ deforms continuously to the original problem $A(u) = f(r)$. The embedding parameter $p \in [0,1]$ can be considered as an expanding parameter [19] to obtain

$$v = v_0 + pv_1 + p^2 v_2 + \ldots. \tag{7}$$

The solution is obtained by taking the limit as p tends to 1 in (7). Hence,

$$u = \lim_{p \to 1} v = v_0 + v_1 + v_2 + \ldots. \tag{8}$$

The series (8) converges for most cases and the rate of convergence depends on $A(u) - f(r)$ [19].

3. Method of Solution

By change of variables, Abel's integral equation (1) reduces to

$$I(\sqrt{y}) = \int_y^1 \frac{\varepsilon(\sqrt{r})}{\sqrt{r-y}} \mathrm{d}r, \quad 0 \le y \le 1,$$

which may be written as

$$I_1(y) = \int_y^1 \frac{\eta(r)}{\sqrt{r-y}} \mathrm{d}r, \text{ where } I_1(y) = I\left(\sqrt{y}\right) \text{ and } \eta(r) = \varepsilon\left(\sqrt{r}\right). \tag{9}$$

To solve (9) by HPM, we consider the following convex homotopy:

$$(1-p)L(r) + p\left[\int_r^1 \frac{L(y)}{\sqrt{y-r}} \mathrm{d}y - I_1(r)\right] = 0. \tag{10}$$

We seek the solution of (10) in the following form:

$$L(r) = \sum_{i=0}^{\infty} p^i L_i(r), \tag{11}$$

where $L_i(r)$, $i = 0, 1, 2, 3, \ldots$, are the functions to be determined. We use the following iterative scheme to evaluate $L_i(r)$. Substituting (11) in (10) and equating the coefficients of p with the same power, one gets

$$\begin{aligned} p^0 &: \quad L_0(r) = 0, \\ p^1 &: \quad L_1(r) = I_1(r), \\ p^2 &: \quad L_2(r) = L_1(r) - \int_r^1 \frac{L_1(y)}{\sqrt{y-r}} \mathrm{d}y, \\ p^3 &: \quad L_3(r) = L_2(r) - \int_r^1 \frac{L_2(y)}{\sqrt{y-r}} \mathrm{d}y, \\ &\vdots \\ p^{n+1} &: \quad L_{n+1}(r) = L_n(r) - \int_r^1 \frac{L_n(y)}{\sqrt{y-r}} \mathrm{d}y. \end{aligned} \tag{12}$$

Hence, the solution of (9) is given by

$$\eta(r) = \lim_{p \to 1} L(r) = \sum_{i=0}^{\infty} L_i(r). \tag{13}$$

4. Numerical Examples

The simplicity and accuracy of the proposed method is illustrated by the following numerical examples by computing the absolute error $E(r) = |\eta(r) - \tilde{\eta}(r)|$, where $\eta(r)$ is the exact solution and $\tilde{\eta}(r)$ is an approximate solution of the problem obtained by truncating the series (13).

Example 1: Consider the Abel integral equation of the first kind

$$\int_y^1 \frac{\eta(r)}{\sqrt{r-y}}\mathrm{d}r = \frac{16}{105}(1-y)^{5/2}(19+72y), \quad \text{for } 0 \le y \le 1, \tag{14}$$

with the exact solution $\eta(r) = (1-r)^2(1+12r)$.

Using (12), we compute the various iterates $L_i(r)$, and they are given as follows:

$$p^0: \quad L_0(r) = 0,$$

$$p^1: \quad L_1(r) = \frac{16}{105}(1-r)^{5/2}(19+72r),$$

$$p^2: \quad L_2(r) = \frac{\pi}{3}(r-1)^3(4+9r) + \frac{16}{105}(1-r)^{5/2}(19+72r),$$

$$\vdots$$

Figures 1 and 2 show the comparison between the exact solution $\eta(r)$ (solid line) and the approximate solution $\tilde{\eta}(r)$ (dotted line) obtained by truncating (13) at the level $n = 32$, and the absolute error $E(r)$, respectively.

The other four examples are different in the sense that their inversions are evaluated using the following form of Abel's integral equation:

$$I_1(y) = \int_0^y \frac{\eta(r)}{\sqrt{y-r}}\mathrm{d}r.$$

Example 2: We now take the following Abel integral equation:

$$\int_0^y \frac{\eta(r)}{\sqrt{y-r}}\mathrm{d}r = \frac{\pi y}{2}, \tag{15}$$

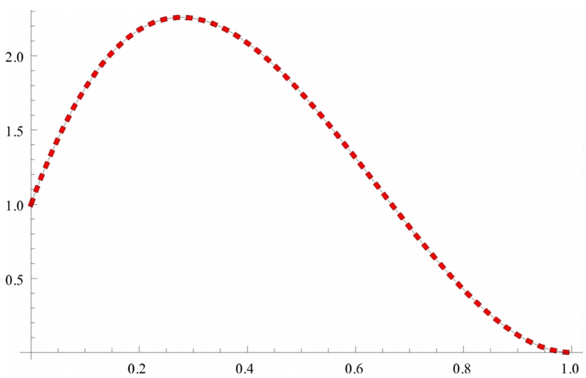

Fig. 1 (colour online). Exact (solid line) and the approximate solution (dotted line) of the Abel integral equation (14) in Example 1.

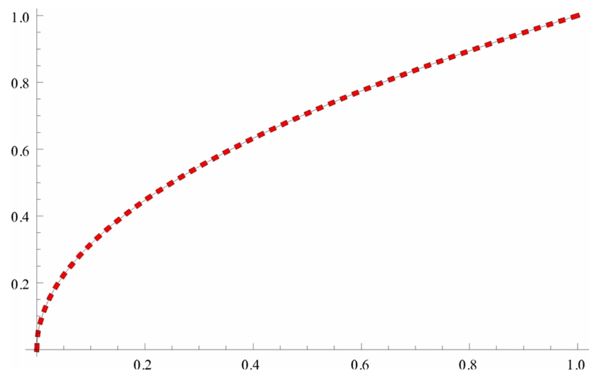

Fig. 3 (colour online). Exact (solid line) and approximate solutions (dotted line) of the Abel integral equation of first kind (15) in Example 2.

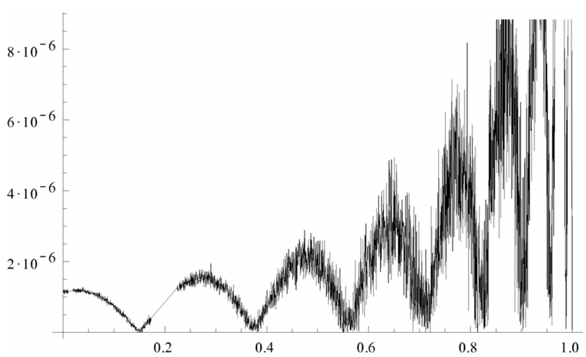

Fig. 2. Absolute error $E(r)$ for Example 1.

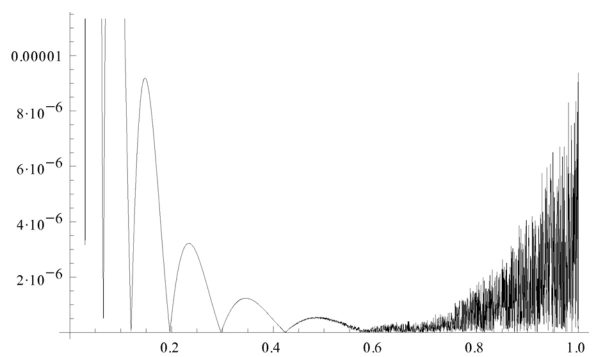

Fig. 4. Absolute error $E(r)$ for Example 2.

with the exact solution $\eta(r) = \sqrt{r}$. The various iterates $L_i(r)$ are given as follows:

$$
\begin{aligned}
p^0:&\quad L_0(r) = 0,\\
p^1:&\quad L_1(r) = \frac{\pi r}{2},\\
p^2:&\quad L_2(r) = \frac{\pi}{3}(r-1)^3(4+9r)\\
p^3:&\quad L_3(r) = \frac{\pi r}{2} - \frac{4\pi r^{3/2}}{3} + \frac{\pi^2 r^2}{4},\\
p^4:&\quad L_4(r) = \frac{\pi r}{2} - 2\pi r^{3/2} + \frac{3\pi^2 r^2}{4} - \frac{4\pi^2 r^{5/2}}{15},\\
&\vdots
\end{aligned}
$$

The series (13) is truncated at level $n = 44$ to obtain Figures 3 and 4 conveying the same information for Example 2 as Figures 1 and 2 did for Example 1.

Example 3: In this example, we consider the following Abel integral equation:

$$\int_0^y \frac{\eta(r)}{\sqrt{y-r}}\mathrm{d}r = \frac{16y^{5/2}}{15}, \tag{16}$$

with the exact solution $\eta(r) = r^2$.

Using (12), we compute the various iterates $L_i(r)$ and they are given as follows:

$$
\begin{aligned}
p^0:&\quad L_0(r) = 0,\\
p^1:&\quad L_1(r) = \frac{16}{15}r^{5/2},\\
p^2:&\quad L_2(r) = \frac{16}{15}r^{5/2} - \frac{\pi r^3}{3},
\end{aligned}
$$

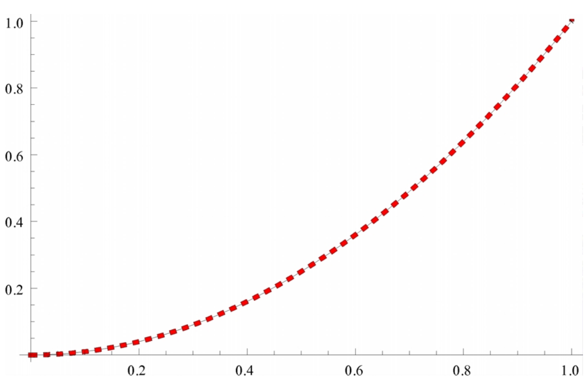

Fig. 5 (colour online). Exact (solid line) and approximate solution (dotted line) of the Abel integral equation of first kind (16) in Example 3.

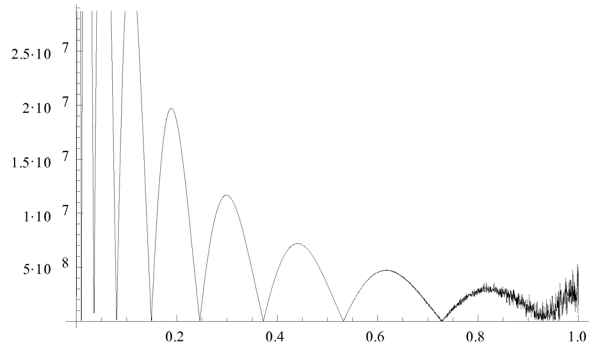

Fig. 6. Absolute error $E(r)$ for Example 3.

$$
\begin{aligned}
p^3:&\quad L_3(r) = \frac{16}{15}r^{5/2} - \frac{2\pi r^3}{3} + \frac{32}{105}\pi r^{7/2},\\
p^4:&\quad L_4(x) = \frac{16}{15}x^{5/2} - \pi x^3 + \frac{32}{35}\pi x^{7/2} - \frac{\pi^2 x^4}{12},\\
&\vdots
\end{aligned}
$$

The corresponding graphs are shown in Figures 5 and 6 with the level of truncation being $n = 36$ for Example 3.

Example 4: Consider the Abel integral equation

$$\int_0^y \frac{\eta(r)}{\sqrt{y-r}}\mathrm{d}r = \frac{8y^{3/2}}{3\sqrt{\pi}}{}_2F_2\left[\left\{\frac{1}{2},1\right\},\left\{\frac{5}{4},\frac{7}{4}\right\},y^2\right], \tag{17}$$

with the exact solution $\eta(r) = \operatorname{erfi}(x)$, where $\operatorname{erfi}(x)$ is the imaginary error function.

The various iterates $L_i(r)$ are given as follows:

$$
\begin{aligned}
p^0:&\quad L_0(r) = 0,\\
p^1:&\ L_1(r) = \frac{8r^{3/2}}{3\sqrt{\pi}}{}_2F_2\left[\left\{\frac{1}{2},1\right\},\left\{\frac{5}{4},\frac{7}{4}\right\},r^2\right],\\
p^2:&\ L_2(r) = -\sqrt{\pi}\left(1 - \mathrm{e}^{r^2} + \sqrt{\pi}r\operatorname{erfi}(x)\right)\\
&\qquad + \frac{8r^{3/2}}{3\sqrt{\pi}}{}_2F_2\left[\left\{\frac{1}{2},1\right\},\left\{\frac{5}{4},\frac{7}{4}\right\},r^2\right],\\
p^3:&\ L_3(r) = -2\sqrt{\pi} + 2\mathrm{e}^{r^2}\sqrt{\pi} + 2\sqrt{\pi r}\\
&\qquad - 2\pi r\operatorname{erfi}(x) - 2\sqrt{\pi r}{}_2F_2\left[\left\{\frac{1}{2},1\right\},\left\{\frac{3}{4},\frac{5}{4}\right\},r^2\right]\\
&\qquad + \frac{32}{15}\sqrt{\pi}x^{5/2}{}_2F_2\left[\left\{\frac{1}{2},2\right\},\left\{\frac{7}{4},\frac{9}{4}\right\},r^2\right]\\
&\qquad + \frac{8r^{3/2}}{3\sqrt{\pi}}{}_2F_2\left[\left\{\frac{1}{2},1\right\},\left\{\frac{5}{4},\frac{7}{4}\right\},r^2\right],\\
&\vdots
\end{aligned}
$$

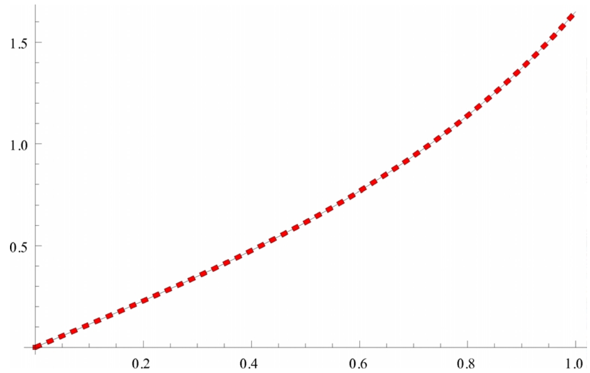

Fig. 7 (colour online). Exact (solid line) and approximate solution (dotted line) of the Abel integral equation of first kind (17) in Example 4.

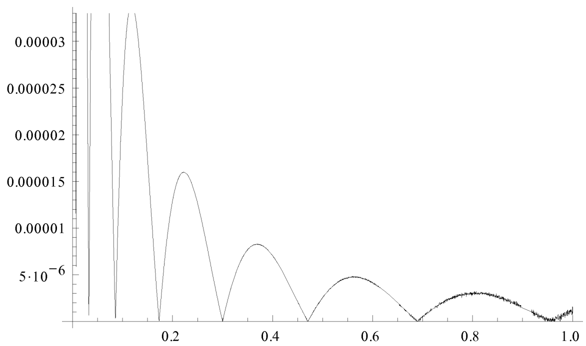

Fig. 8. Absolute error $E(r)$ for Example 4.

We have drawn Figures 7 and 8 by taking $n = 28$ for Example 4.

Example 5: Consider the Abel integral equation of the first kind

$$\int_0^y \frac{\eta(r)}{\sqrt{y-r}}\mathrm{d}r = \frac{\pi\sqrt{y}J_{3/4}\left(\frac{y}{2}\right)J_{5/4}\left(\frac{y}{2}\right)}{\sqrt{2}}, \tag{18}$$

with the exact solution $\eta(r) = J_2(r)$, where $J_2(r)$ is the Bessel function of the first kind. The various iterates $L_i(r)$ are given as follows:

$$p^0:\ L_0(r) = 0,$$

$$p^1:\ L_1(r) = \frac{\pi\sqrt{r}J_{3/4}\left(\frac{r}{2}\right)J_{5/4}\left(\frac{r}{2}\right)}{\sqrt{2}},$$

$$p^2:\ L_2(r) = \frac{\pi\sqrt{r}J_{3/4}\left(\frac{r}{2}\right)J_{5/4}\left(\frac{r}{2}\right)}{\sqrt{2}} - \frac{\pi r^3}{24}\,{}_1F_2\left[\left\{\frac{3}{2}\right\},\left\{\frac{5}{2},3\right\},-\frac{r^2}{4}\right],$$

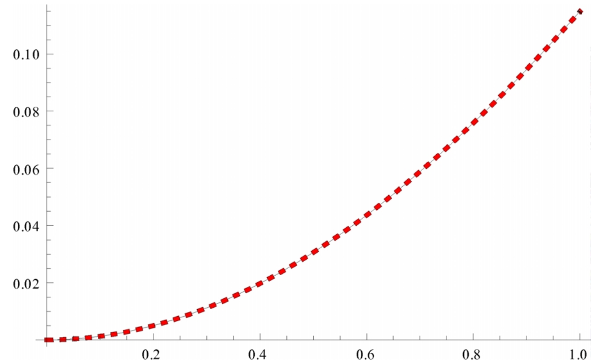

Fig. 9 (colour online). Exact (solid line) and approximate solution (dotted line) of the Abel integral equation of first kind (18) in Example 5.

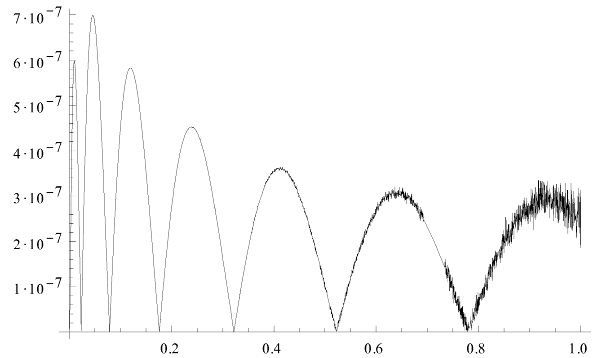

Fig. 10. Absolute error $E(r)$ for Example 5.

$$p^3:\ L_3(r) = -\frac{2\pi}{\sqrt{r}} + \frac{\pi\sqrt{r}J_{3/4}\left(\frac{r}{2}\right)J_{5/4}\left(\frac{r}{2}\right)}{\sqrt{2}} + \frac{2\pi}{\sqrt{r}}\,{}_1F_2\left[\left\{-\frac{1}{2}\right\},\left\{\frac{1}{4},\frac{3}{4}\right\},-\frac{r^2}{4}\right] - \frac{4}{3}\pi r^{3/2}\,{}_1F_2\left[\left\{\frac{1}{2}\right\},\left\{\frac{5}{4},\frac{7}{4}\right\},-\frac{r^2}{4}\right] - \frac{\pi r^3}{12}\,{}_1F_2\left[\left\{\frac{3}{2}\right\},\left\{\frac{5}{2},3\right\},-\frac{r^2}{4}\right],\ldots.$$

Calculating the terms up to $L_{23}(r)$, we have drawn the Figures 9 and 10 showing the comparison and the absolute error between the exact and approximate solutions respectively for Example 5.

5. Conclusions

From the given numerical examples and the Figures 1 – 10, we conclude that the HPM is a very powerful and simple tool for solving Abel's integral equations of the first kind.

Acknowledgements

The first author acknowledges the financial support from Rajiv Gandhi National Fellowship of the University Grant Commission, New Delhi, India under the JRF scheme.

The authors would like to thank the anonymous referees for their helpful comments.

[1] N. H. Abel, J. Reine Angew. Math. **1**, 153 (1826).
[2] L. Mach, Wien Akad. Ber. Math. Phys. Klasse **105**, 605 (1896).
[3] F. G. Tricomi, Integral Equations, Interscience, New York 1975.
[4] G. N. Minerbo and M. E. Levy, SIAM J. Numer. Anal. **6**, 598 (1969).
[5] M. Deutsch and I. Beniaminy, Appl. Phys. Lett. **41**, 27 (1982).
[6] M. Deutsch, Appl. Phys. Lett. **42**, 237 (1983).
[7] S. A. Yousefi, Appl. Math. Comput. **175**, 574 (2006).
[8] I. Beniaminy and M. Deutsch, Comput. Phys. Commun. **27**, 415 (1982).
[9] D. A. Murio, D. G. Hinestroza, and C. E. Mejia, Comput. Math. Appl. **23**, 3 (1992).
[10] S. Bhattacharya and B. N. Mandal, Appl. Math. Sci. **2**, 1773 (2008).
[11] S. Ma, H. Gao, L. Wu, and G. Zhang, J. Quant. Spectrosc. Radiat. Transfer **109**, 1745 (2008).
[12] S. Ma, H. Gao, G. Zhang, and L. Wu, J. Quant. Spectrosc. Radiat. Transfer **107**, 61 (2007).
[13] O. P. Singh, V. K. Singh, and R. K. Pandey, Int. J. Nonlinear Sci. Numer. Simul. **10**, 681 (2009).
[14] O. P. Singh, V. K. Singh, and R. K. Pandey, J. Quant. Spectrosc. Radiat.Transfer **111**, 245 (2010).
[15] D. D. Ganji and A. Rajabi, Int. Commun. Heat Mass Tranfer **33**, 391 (2006).
[16] J. H. He, Int. J. Nonlinear Mech. **34**, 699 (1999).
[17] S. J. Liao, Int. J. Nonlinear Mech. **30**, 371 (1995).
[18] S. J. Liao, Eng. Anal. Boundary Element **20**, 91 (1997).
[19] J. H. He, Comput. Meth. Appl. Mech. Eng. **178**, 257 (1999).
[20] J. H. He, Int. J. Nonlinear Mech. **35**, 37 (2000).
[21] C. Hillermeier, Int. J. Optim. Theory Appl. **110**, 557 (2001).
[22] J. H. He, Commun. Nonlinear Sci. Numer. Simul. **3**, 92 (1998).
[23] J. H. He, Appl. Math. Comput. **151**, 287 (2004).
[24] J. H. He, Appl. Math.Comput. **156**, 527 (2004).
[25] D. D. Ganji, G. A. Afrouzi, H. Hosseinzadeh, and R. A. Talarposhti, Phys. Lett. A **371**, 20 (2007).
[26] J. H. He, Int. J. Nonlinear Sci. Numer. Simul. **1**, 51 (2000).